Journal of Solid State Chemistry **142,** 428–439 (1999)
Article ID jssc.1998.8058, available online at http://www.idealibrary.com on IDEAL®

First Principles Hartree–Fock Description of Lithium Insertion in Oxides

I. The End Members TiO_2 and $LiTiO_2$ of the System Li_xTiO_2

W. C. Mackrodt

School of Chemistry, University of St. Andrews, St. Andrews, Fife KY16 9ST, United Kingdom
E-mail: wcm@st-and.ac.uk

Received June 22, 1998; in revised form October 6, 1998; accepted October 9, 1998

First principles periodic Hartree–Fock calculations are reported for the $P4_2/mnm$ (rutile), $I4_1/amd$ (anatase), $Pbca$ (brookite), $Pnma$ (ramsdellite), $Pcbn$ (colombite), $Fd\bar{3}m$ (spinel), and $Imma$ (orthorhombic) polymorphs of TiO_2, from which the predicted order of stability is

$$P4_2/mnm > I4_1/amd > Pbca \approx Pcbn > Pnma > Imma > Fd\bar{3}m.$$

The calculated difference in energy between the rutile and anatase structures is 0.02–0.06 eV, in good agreement with a recent local density approximation (LDA) estimate of 0.033 eV and an experiment enthalpy difference of 0.05 eV. The corresponding Hartree–Fock and LDA differences for the brookite structure are 0.06 and 0.058 eV, respectively. The calculated volumes, which are based on isotropic volume-optimized Hartree–Fock energies, are also in good agreement with recent LDA calculations and with experiment. Spin-unrestricted calculations are reported for the $Fm\bar{3}m$, $Imma$, $Pnma$, and $P4_2/mmm$ of $LiTiO_2$, where the stability is in the order

$$Imma > Fm\bar{3}m > Pnma > P4_2/mnm.$$

The only reported phase for $LiTiO_2$ is $Fm\bar{3}m$, for which the calculated volume is in good agreement with experiment. From the relative stabilities of TiO_2 and $LiTiO_2$, the relative lithium insertion potentials corresponding to $TiO_2 \xrightarrow{Li} LiTiO_2$ are deduced, with a maximum variation of 1.6 eV for the different polymorphic routes. The maximum voltage predicted is that for the $Imma$ route which is $\sim$1 eV larger than that for $Pnma$. Direct comparisons with the calculated energy for $C2/m$ $Li_{0.5}MnO_2 \xrightarrow{Li} LiMnO_2$ lead to an estimate of the voltage for $Imma$ $TiO_2 \xrightarrow{Li} LiTiO_2$ of $\sim$1.3 eV, which is $\sim$2.5 eV *anodic* to the Mn system. The corresponding values for the $Pnma$ polymorphic route are $\sim$3 and $\sim$3.5 eV, respectively. Mulliken population analyses indicate that lithium is completely ionized in $LiTiO_2$ and that the charge transfer is predominantly to the oxygen sublattice. There is a rehybridization of the titanium valence orbitals leading to a slight increase in the 3*d* population and strong localization of spin density at the titanium sites with local moments of $\sim 1\ \mu_B$. © 1999 Academic Press

1. INTRODUCTION

In recent years there has been considerable interest in the development of lithium-insertion solid state batteries as portable power sources (1,2). While this development is largely technologically driven at present, as elsewhere in solid state chemistry (3), a fundamental understanding of the structural, energetic, and electronic properties of these materials is likely to facilitate further progress in this important area of research. It is now widely accepted that computer-based theoretical methods can contribute to this understanding in the form of insight and, in some cases, data, which complements that obtained from experiment. Of the methods now available, those based on first principles electronic structure calculations show particular promise and have been used recently in studies of Li(Co,Al)O_2 (4) and $C2/m$ Li_xMnO_2 (5), the cathodic properties of which Armstrong and Bruce had demonstrated earlier in a lithium "rocking-chair" system (6). The study of Li_xMnO_2 (5) was based on the spin-unrestricted periodic Hartree–Fock (UHF) method, which a number of studies have shown to give a good description of the ground state properties of magnetic insulators (7–12). In particular, the study of $C2/m$ Li_xMnO_2 (5) demonstrated the versatility of the UHF method in that it provided both a fundamental description of the changes in the electronic and magnetic structures associated with lithium insertion and an accurate account of electrode properties such as the constancy of the voltage with x and the effects of cation disorder. Furthermore, it suggested that oxygen k-edge spectroscopy might provide a useful tool for investigating changes in valence state as a function of lithium content, as in the seminal study of $Li_xNi_{1-x}O$ by Kuiper *et al.* (13). For in agreement with previous UHF studies of NiO (7,9), MnO (11), and MnO_2 (14), it found that changes in the formal valence state from Mn(III) to Mn(IV) are associated largely with the oxygen sublattice, as opposed to the

0022-4596/99 $30.00

conventional Mott-Hubbard description in terms of Mn^{3+} and Mn^{4+}.

In the present paper a similar approach based on the UHF method is used to study the polymorphs of TiO_2 and $LiTiO_2$ as a prelude to a fuller investigation of the system, Li_xTiO_2. Akimoto *et al.* (15) have prepared the ramsdellite phase of Li_xTiO_2 in the range $(0 \leq x \leq 0.45)$ and, more recently, Gover *et al.* (16) have measured the electrochemical properties of this phase. While the operational cathodic range of stoichiometry, x, may be less than $(0 < x < 1)$, a study of the end members provides important clues as to the properties and behavior of the intervening region. The objectives here are threefold: first, to extend a previous study of $C2/m$ Li_xMnO_2 to the lithiation of TiO_2 and, in particular, to compare the fundamental electronic (and magnetic) processes therein; second, to study the structural, energetic, and electronic changes associated with the lithiation of TiO_2 to $LiTiO_2$; and third, to investigate the sensitivity of the calculated voltage (lithiation energy) to (small) variations in the structures of the various polymorphs as between experiment and calculation. The significance of the latter is that it is unlikely that complete energy-minimized structures within the entire system, Li_xTiO_2, can be obtained, so that in many cases the calculation of lithiation energies will be restricted to approximate structures. Here a particular subset of approximate structures is examined, namely those obtained by minimizing the UHF energy with respect to isotropic variation of the unit cell volume. Structures of this type might reasonably be obtained for the entire Li_xTiO_2 system while volume changes associated with lithium insertion are likely to be a practical consideration in the use of this and other systems as electrodes. Lithiation can result in large changes in volume and also vary appreciably from one polymorph to another. Thus, there is an increase in volume of 14.6, 12.6, and 13.7% from $P4_2/mnm$ TiO_2 to $Pnma$ $Li_{0.5}TiO_2$, $Imma$ $Li_{0.5}TiO_2$ and $Fm\bar{3}m$ $LiTiO_2$, respectively, whereas the lithiation of $Pnma$ TiO_2 to $Pnma$ $Li_{0.5}TiO_2$ results in a volume increase of only 4.3%. Even larger changes occur for MnO_2, where the difference in volume between $P4_2/mnm$ MnO_2 and $C2/m$ $LiMnO_2$, for example, is 33.5%. In the absence of full structural optimization, therefore, sensible estimates of changes in volume should provide a reasonable basis for estimating voltages associated with lithum insertion in TiO_2 and other systems.

2. THEORETICAL PROCEDURES

The all-electron *ab initio* LCAO Hartree–Fock method for periodic systems and its computational implementation in the CRYSTAL 95 computer code (17) have been described in detail previously (18). The calculations reported here use extended Gaussian basis sets and are based on the spin unrestricted (UHF) procedure (19) to describe open-shell electronic configurations. The numerical values of the tolerance parameters involved in the evaluation of the (infinite) Coulomb and exchange series were identical to those used in recent studies (8): a detailed account of the effect of these tolerances is discussed elsewhere (20). The reciprocal space integration utilized the Monkhorst–Pack sampling (21), with shrinking factors that gave a minimum of 36 k-points in the IBZ, and the SCF convergence criterion based on differences in the total energy of the unit cell of less than 10^{-6} Ha. *A posteriori* corrections for electron correlation based on three generalized gradient approximations are included in the present study: they are due to Perdew (22), Perdew and Wang (23), and Perdew *et al.* (23), referred to as P, PW, and PBE, respectively. The localized crystal orbitals consisted of 25 atomic orbitals for Ti, 7 for Li, and 14 for O of the type

Ti: $1s(8)2sp(6)3sp(4)4sp(1)5sp(1)3d(4)4d(1)$

Li: $1s(6)2sp(1)$

O: $1s(8)2sp(4)3sp(1)4sp(1)$

where the numbers in parenthesis are the numbers of Gaussian functions used to describe the corresponding shell, e.g., $1s$, $2sp$, $3d$, etc. The basis set for Ti is a $[\ldots]3d(3)$ to $[\ldots]3d(4)4d(1)$ expansion of that used previously in a study of electron-excess states in TiO_2 (25). The exponents and contraction coefficients for Ti and O are those used in this latter study (26) and for those for Li taken from studies of Li : NiO (9) and $LiMnO_2$ (5): here they have been used unchanged for $LiTiO_2$.

Isotropic variation of the unit cell volume to obtain the minimum UHF energy is carried out by varying the matrix of fundamental vectors, $\mathbf{L}$ (17),

$$\mathbf{L} = \begin{bmatrix} \vec{l}_1 \\ \vec{l}_2 \\ \vec{l}_3 \end{bmatrix},$$

as

$$\mathbf{L}' = (\mathbf{I} + \varepsilon)\mathbf{L}$$

using the symmetric elastic tensor, ε,

$$\varepsilon = \begin{pmatrix} \delta & 0 & 0 \\ 0 & \delta & 0 \\ 0 & 0 & \delta \end{pmatrix}$$

with

$$V = \det(\mathbf{L}))$$

such that

$$\partial E_{\mathrm{UHF}}/\partial\delta = 0,$$

where E_{UHF} is the total UHF energy. The corresponding structures are thus isotropic volume-optimized Hartree–Fock structures and for the purposes of this paper will be referred to simply as the "Hartree–Fock" structures.

Following previous studies of Li : NiO (9), MnO (11), and $C2/m$ $LiMnO_2$ (5), the principal quantities that are used to examine the nature of the valence states in the various polymorphs of TiO_2 and $LiTiO_2$ are the Mulliken charge and spin populations (27) and densities of (single particle) states (DOS). As emphasized before (9), while the Mulliken charge is defined in terms of the particular basis set used and is only a *guide* to the total electron density at a given atomic site, *differences* in the Mulliken charge resulting from structural changes or the addition or removal of electrons are a reasonable measure of the *change* in the electron density, and it is precisely this change that is of interest here.

3. RESULTS

3.1. TiO_2

Crystal structures for five polymorphs of TiO_2 have been reported with $P4_2/mnm$ (rutile) (28), $I4_1/amd$ (anatase) (28), *Pbca* (brookite) (29), *Pnma* (ramsdellite) (15), and *Pcbn* (colombite) (30) symmetries. They are shown schematically in Figs. 1–5, where regions of void, suitable for lithium insertion, are evident. *Pcbn* is a high-pressure phase which can be prepared from rutile, anatase, or brookite. The higher pressure $P2_1/c$ (baddeleyite) phase is not considered in this study. Details of the unit cell volumes are collected in Table 1, where the volume for *Pcbn* is that measured at 40 kbar and 450°C (30). Also included in Table 1 are the *Imma* and $Fd\bar{3}m$ structures of $Li_{0.5}TiO_2$ reported by Cava *et al.* (31): the former is shown in Fig. 6, where, again, open channels, suitable for lithium insertion, are evident. Thus there are variations in the volumes of the known polymorphs of TiO_2 of up to $\sim$10%, which is comparable to the difference in volume between $P4_2/mnm$ TiO_2 and *Imma* $Li_{0.5}TiO_2$ and twice that between *Pnma* TiO_2 and *Pnma* $Li_{0.5}TiO_2$ (15). For comparison, Table 2 shows that even larger variations in volume have been reported for the polymorphs of MnO_2, so that TiO_2 is not unique in this respect.

As reported previously for the rutile phase (25), UHF and spin-restricted (RHF) calculations lead to identical insulating, nonmagnetic ground states for all seven polymorphs in both the experimental and Hartree–Fock structures. Starting with the experimental structures, Table 3 contains the

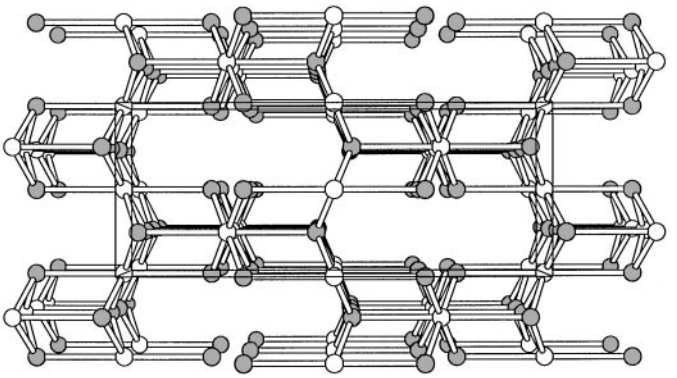

FIG. 2. Anatase ($I4_1/amd$) structure viewed down the *a* axis.

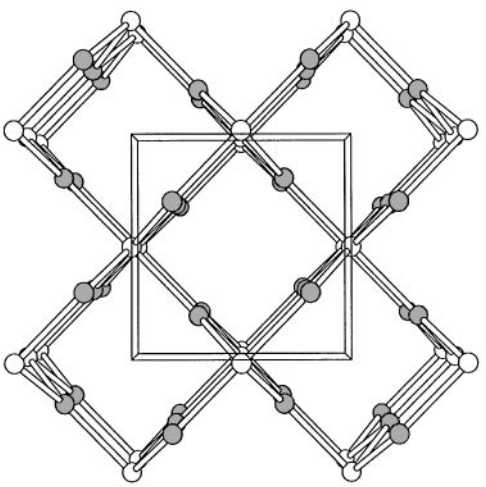

FIG. 1. Rutile ($P4_2/mnm$) structure viewed down the *c* axis (white circles, titanium; grey circles, oxygen).

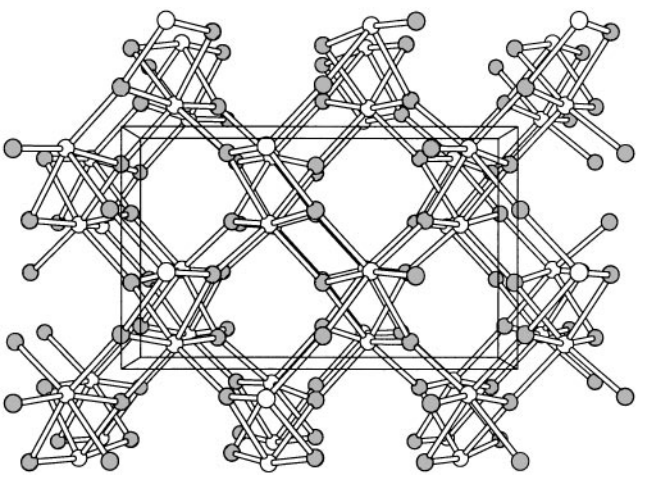

FIG. 3. Brookite (*Pbca*) structure viewed down the *c* axis.

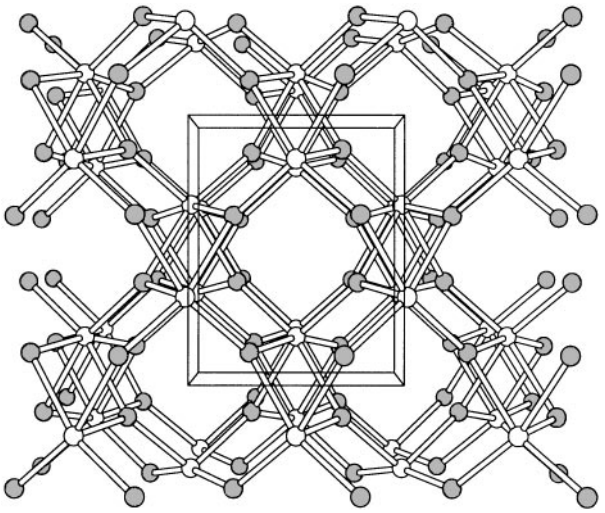

FIG. 4. Colombite (*Pcbn*) structure viewed down the *c* axis.

TABLE 1
Comparison of the Experimental Volumes (Å^3) of the Polymorphs of TiO_2

Structure	Space group	Sp.gp.no.	Ref.	Volume	Δv (%)
Rutile	$P4_2/mnm$	136	28	31.2175	0.0
Anatase	$I4_1/amd$	141	28	34.0670	+9.13
Brookite	*Pbca*	61	29	32.1055	+2.84
Ramsdellite	*Pnma*	62	15	34.2964	+9.86
Columbite	*Pbcn*	60	30	30.6452	−1.87
Orthogonal	*Imma*	74	31	35.1360	+12.55
Spinel	$Fd\bar{3}m$	227	31	37.0877	+18.80

Note. For the *Imma* and $Fd\bar{3}m$ structures the volumes are those of $Li_{0.5}TiO_2$ (31).

total RHF energy per formula unit of $P4_2/mmm$ TiO_2 (25) together with corrections based on the PBE, PW and P correlation-only functionals. From this it is clear that *a posteriori* corrections of this type give only a rough estimate of the *total* correlation energy, with differences between the three functionals in excess of 1 Ha per formula unit. However, as Table 4 shows, *differences* in energy, here the energies of the various polymorphs of TiO_2 relative to the energy of $P4_2/mnm$, are very much closer, and less than 0.2 eV for the four approximations. As a further guide to the stability of TiO_2 with respect to structure, Table 5 contains the relative RHF and RHF/PBE energies of TiO_2 based on the structures of *Pnma* Li_xTiO_2 ($0 \leq x \leq 0.45$) reported by Akimoto *et al.* (15).

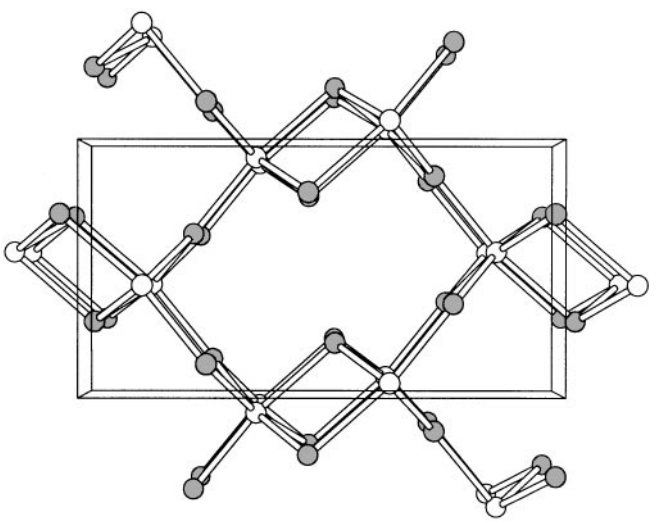

FIG. 5. Ramsdellite (*Pnma*) structure viewed down the *b* axis.

Turning now to the Hartree–Fock structures, Table 6 contains the calculated Hartree–Fock volumes of the various polymorphs of TiO_2, their differences compared with experiment, δv, and their values relative to the RHF $P4_2/mnm$ structure, Δv. Also given in Table 6 are the UHF volume and δv of $P4_2/mnm$ MnO_2 for comparison. Table 7 lists the relative energies of the Hartree–Fock structues, and Table 8 lists the differences in total energy per formula unit of TiO_2 between the Hartree–Fock and experimental structures together with those for $P4_2/mnm$ MnO_2, again for comparison. Finally in this subsection, Table 9 compares the Mulliken charges, q_M, and 3*d* populations, n_d, of the Hartree–Fock structures of various polymorphs of TiO_2. The corresponding values for the experimental structures are identical.

3.2. $LiTiO_2$

The only experimental structure of $LiTiO_2$ appears to be that of Lecerf (35), who reported a disordered $Fm\bar{3}m$ phase with a lattice constant of 4.14 Å. As an approximation to

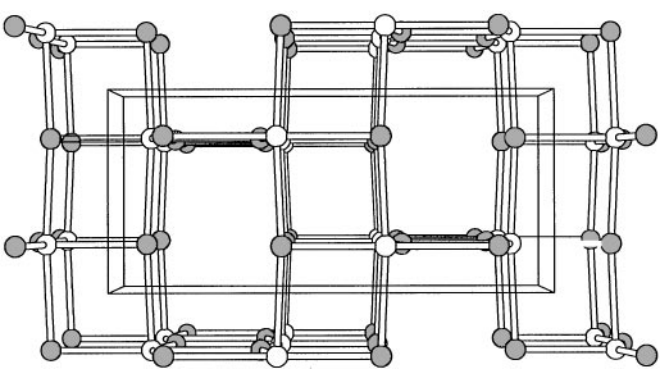

FIG. 6. Orthorhombic (*Imma*) structure viewed down the *a* axis.

TABLE 2
Comparison of the Experimental Volumes (Å^3) of the Polymorphs of MnO_2

Space group	Sp.gp.no.	Ref.	Volume	Δv (%)
$P4_2/mnm$	136	32	27.8964	0.0
Pnma	62	33	29.5627	+5.97
*I*4/*m*	87	33	34.2829	+22.89

TABLE 3
The Calculated Total Energies (Ha) of the $P4_2/mnm$ Structure of TiO_2 (28)

Approximation	Energy
RHF	−998.387926
RHF/PBE	−999.895516
RHF/PW	−1001.320982
RHF/P	−1000.015098

Note. Here and in all subsequent tables, energies are per formula unit.

this state, *ordered* structures built from single, double, and quadruple unit cells have been examined. They lead to essentially identical states, so that here the results for the double unit cell only are given here. There are also reported structures of $Li_{0.5}TiO_2$ in *Imma* and $Fd\bar{3}m$ symmetries by Cava *et al.* (31) and *Pnma* symmetry by Akimoto *et al.* (15). From these, *Imma* and *Pnma* structures for $LiTiO_2$ can be constructed readily by assuming full occupancy of the lithium positions, as shown in Figs. 7 and 8. A high-symmetry structure derived from $P4_2/mnm$ TiO_2 can also be constructed by lithium insertion at ($a/2$, 0 $c/2$) and (0, $a/2$, $c/2$). For convenience, these strucures, whose volumes are those of $L_{0.5}TiO_2$ (*Imma* and *Pnma*) and TiO_2 ($P4_2/mnm$), are referred to as "experimental" structures. Thus four polymorphs of $LiTiO_2$ are examined in this introductory paper, leaving others, which require more extensive structural optimization, for future reports.

As found previously for the electron-excess structure of oxygen-deficient $P4_2/mnm$ TiO_2 (25), the RHF solutions for all four polymorphs of $LiTiO_2$ considered here are conducting. They are also higher in energy than the UHF solutions by over 3 eV and, as a result, have not been investigated further. Of the experimental structures, *Imma* is lowest in energy both at the UHF and *a posteriori* corrected levels of approximation: accordingly, the energies of the other structures are measured against these values, which are given in Table 10. With the exception of the *Imma* structure, attention here is confined to the ferromagnetic solutions of $LiTiO_2$, for, as shown elsewhere (5, 7, 9, 11), differences in spin configuration have only a minor effect on the overall electronic structure and are likely to make an insignificant contribution to insertion voltages. As in the case of $P4_2/mnm$ TiO_2, estimates of the total correlation energy differ by in excess of 1 Ha, so that, again, they are largely a guide to the order of magnitude, which for both systems is ~0.1% of the total. However, as Table 11 shows, the *relative* energies of the four structures are again much closer, with differences between the four approximations of less than 0.2 eV. Hartree–Fock volumes are given in Table 12, and while comparison with experiment is valid, strictly speaking, only for the $Fm\bar{3}m$ structure, for completeness, values of δv are included for the other structures. Also included, for comparison, is the value for $C2/m$ $LiMnO_2$ (6). Table 13 contains the relative energies per formula unit of the four polymorphs of $LiTiO_2$, and Table 14 shows the differences in energy between the experimental and Hartree–Fock structues. Again, strictly speaking, these differences are meaningful only for the $Fm\bar{3}m$ structure, but are an integral part of this paper.

Turning now the electronic structure of $LiTiO_2$, Table 15 compares the Mulliken charges, q_M, 3d populations, n_d, and local spin moments, n_s, of the Hartree–Fock structures, and Table 16 shows the *changes* in these quantities compared with TiO_2. These changes effectively describe the electronic (and magnetic) processes involved in lithium insertion into TiO_2 and are fundamental to an understanding of the physics and chemistry of lithium insertion electrodes. Furthermore, as discussed in the following section, UHF calculations suggest that the electronic processes associated with lithium insertion in TiO_2 differ subtly from those in MnO_2 (5), and it is precisely these differences that are of the interest in understanding the fundmantal processes of lithium insertion in oxides. Table 17 compares lithium insertion energies for different initial and final polymorphic phases based on their Hartree–Fock structures, and Table 18 shows energies of the competitive lithiation/delithiation of TiO_2/($C2/m$) $LiMnO_2$ for these initial and final phases. These latter energies correspond

TABLE 4
Comparison of the Relative Energies (eV) of the Polymorphs of TiO_2 for the Experimental Structures

Space group	Δv (%)	RHF	PBE	PW	P
$P4_2/mnm$	0.0	0.0	0.0	0.0	0.0
$I4_1/amd$	+9.13	−0.002	+0.05	$+0.00_6$	$+0.05_6$
Pbca	+2.84	+0.04	+0.06	+0.05	+0.06
Pnma	+9.86	+0.57	+0.59	+0.62	+0.66
Pbcn	−1.87	+0.03	−0.02	+0.01	−0.02
Imma	+12.55	+0.66	+0.77	+0.72	+0.77
$Fd\bar{3}m$	+18.80	+1.81	+1.96	+1.93	+1.96

TABLE 5
Relative RHF and RHF/PBE Energies (eV) of TiO_2 Based on the Structures of *Pnma* Li_xTiO_2 (15) as a Function of x and Volume (Å^3)

x	Volume	Δv (%)	RHF	PBE
0.0	34.2964	0.0	0.0	0.0
0.14	35.1014	+2.35	+0.05	+0.10
0.16	35.1727	+2.56	+0.06	+0.11
0.41	35.6476	+3.94	+0.20	+0.31
0.45	35.7726	+4.30	+0.23	+0.36

TABLE 7
Comparison of the Relative Energies (eV) of the Polymorphs of TiO_2 for the Hartree–Fock Structures

Space group	RHF	PBE	PW	P
$P4_2/mnm$	0.0	0.0	0.0	0.0
$I4_1/amd$	+0.02	+0.06	$+0.01_5$	+0.06
Pbca	+0.06	+0.06	+0.06	+0.06
Pnma	+0.58	+0.59	+0.59	+0.60
Pbcn	+0.05	$+0.00_4$	+0.03	$+0.00_5$
Imma	+0.66	+0.67	+0.66	+0.67
$Fd\bar{3}m$	+1.78	+1.73	+1.79	+1.74

directly to the (open cell) cathodic voltage difference between Li_xTiO_2 and $C2/m$ Li_yMnO_2 in the ranges, x: $0 \rightarrow 1$ and y: $1 \rightarrow 0.5$.

4. DISCUSSION

Since this study is concerned with a Hartree–Fock description of the structure, energetics, and electronic processes associated with lithium insertion in TiO_2, it is essential to verify that the RHF/UHF method gives a qualitatively correct description of the electronic structures and relative stabilities of the most stable phases. Starting with the five known polymorphs and the hypothetical *Imma* and spinel structures derived from the data of Cava *et al.* for $Li_{0.5}TiO_2$ (31), they are all predicted to be insulating, nonmagnetic, partially covalent systems, which agrees with the known properties of the rutile ($P4_2/mnm$), anatase ($I4_1/amd$), and brookite (*Pcba*) phases (36), with no indications that either the high-pressue (*Pcbn*) or ramsdellite (*Pnma*) phases are any different (15, 30). Table 4 shows that the RHF and *a posteriori* corrected energies of the experimental structures of the $P4_2/mnm$, $I4_1/amd$, *Pbca*, and *Pbcn* polymorphs are within 0.06 eV (~700 K) with the *Pnma* and *Imma* structures less stable by ~0.6 eV and the $Fd\bar{3}m$ structure by ~1.9 eV. At the RHF level of approximation the rutile and anatase phases are predicted to be very close in energy despite a difference in volume of ~9.9%, with the rutile phase stabilized by a lower correlation energy as a result of its reduced volume. These results also suggest that the high-pressure phase is also stabilized by correlation energy effects associated with its low volume. Akimoto *et al.* (15) have reported a ramsdellite-to-brookite transformation above 640 K, so that, overall, a Hartree–Fock description of the relative stabilities of the experimental structures of TiO_2 would seem to be consistent with the known data. Further evidence of this qualitatively correct description of phase stability is contained in Table 5, which confirms that the lowest energy *Pnma* structure of TiO_2 within the range of reported Li_xTiO_2 structures (15) is indeed that for $x = 0$. In addition, it gives a first estimate of the sensitivity of RHF energies to deviations/uncertainties in structure with an increases of 0.05 and 0.20 eV in the energy of TiO_2 based on the structures of $Li_{0.14}TiO_2$ and $Li_{0.41}TiO_2$, respectively.

Turning now to the (volume-optimized) Hartree–Fock structures of TiO_2, Table 6 shows that the calculated

TABLE 6
Comparison of the Hartree–Fock Volumes (Å^3) of the Polymorphs of TiO_2, Δv(%), with Experiment, δv(%), and Those of Ref. (37)

Space group	Volume	δv (%)	Δv (%)	Ref. (37)
$P4_2/mnm$	31.4760	+0.83	0.0	31.535
$I4_1/amd$	34.3139	+0.73	+9.02	35.009
Pbca	32.2695	+0.51	+2.52	32.611
Pnma	33.9436	−1.03	+7.84	—
Pbcn	30.9774	+1.08	−1.58	30.855
Imma	33.0697	−5.88	+5.06	—
$Fd\bar{3}m$	35.4436	−4.43	+12.61	—
$P4_2/mnm$ MnO_2	27.7034	−0.69	—	—

Note. Also given is the volume and δv for $P4_2/mnm$ MnO_2.

TABLE 8
Differences in Energy (eV) between the Experimental and Hartree–Fock Structures of the Polymorphs of TiO_2

Space group	RHF	PBE	PW	P
$P4_2/mnm$	−0.02	+0.02	$+0.00_4$	+0.02
$I4_1/amd$	-0.00_1	+0.03	+0.01	+0.02
Pbca	$+0.00_4$	+0.02	+0.01	+0.02
Pbcn	$+0.00_1$	+0.04	+0.02	+0.04
Pnma	-0.00_4	+0.03	−0.02	−0.04
$P4_2/mnm$ MnO_2	−0.04	−0.06	−0.05	−0.06

Note. Also given are the differences for $P4_2/mnm$ MnO_2.

TABLE 9
Comparison of Mulliken Charges, $q_M(x)$ (e), and 3d Populations, n_d, of the Polymorphs of TiO_2 for the Hartree–Fock Structures

Space group	q_M(Ti)	$q_M(O_1)$	$q_M(O_2)$	n_d
$P4_2/mnm$	2.49	1.24	—	1.25
$I4_1/amd$	2.43	1.22	—	1.30
Pbca	2.44	1.26	1.18	1.30
Pnma	2.35	1.25	1.10	1.37
Pbcn	2.50	1.25	—	1.24
Imma	2.32	1.10	1.21	1.39

volumes of the five known polymorphs, including the high-pressure *Pbcn* and high-energy *Pnma* phases, are within 1.1% of the experimental values. For comparison the value for rutile MnO_2 is $\sim$0.7%. The volume of the (hypothetical) *Imma* structure, 33.07 Å^3, is predicted to lie between those of the brookite and ramsdellite structures and $\sim$5.9% less than that of *Imma* $Li_{0.5}TiO_2$. As expected the spinel structure is found to be the least dense, with a predicted volume of 35.44 Å^3, or $\sim$12.6% greater than the rutile phase. Both the pattern and magnitudes of the relative energies of the six phases, given in Table 7, are very similar to those for the experimental structures (Table 2), with the rutile structure now lowest in energy at both the RHF and all *a posteriori* corrected levels of approximation. The anatase, brookite, and high-pressure phases are all $\leq$ 0.06 eV above rutile with the ramsdellite and *Imma* structures again $\sim$0.6 eV and the spinel structure $\sim$1.8 eV more energetic.

The single discrepancy with the known phase stability is that the equilibrium (zero pressure) colombite phase is predicted to be 0.01 eV more stable than brookite, which is qualitatively incorrect, for colombite is a high-pressure phase. The most likely reason for this is the approximate

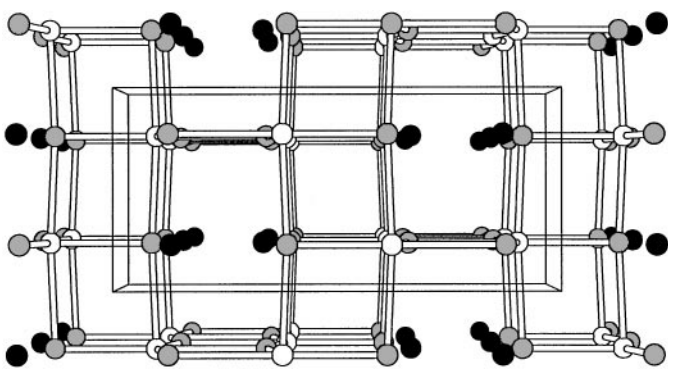

FIG. 7. Orthorhombic (*Imma*) structure of $LiTiO_2$ viewed down the *a* axis (black circles, lithium).

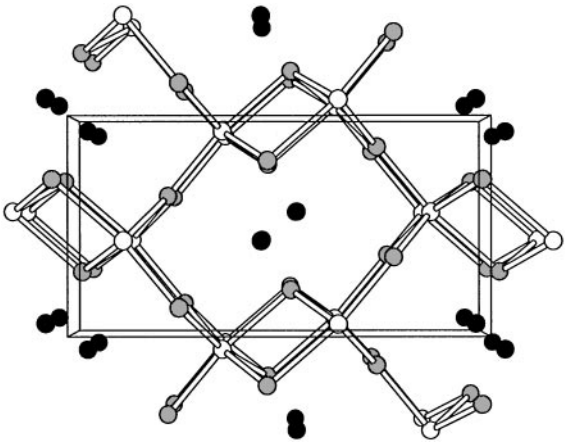

FIG. 8. Ramsdellite (*Pnma*) structure of $LiTiO_2$ viewed down the *b* axis.

nature of the volume optimization used in the present study. However, what is particularly significant within the context of this paper is that differences in the relative RHF energies between the two sets of structures are $\leq$ 0.02 eV for all seven polymorphs, as shown in Table 8. This compares with a value of 0.04 eV for rutile MnO_2.

The results presented here are in remarkably good agreement with those reported recently by Milman (37) based on the local density approximation (LDA) as implemented in the CASTEP computer code. With regard to theoretical volumes, the two sets of calculations agree to within 1% for the rutile, brookite, and colombite phases and to within 2% for anatase. This is particularly satisfying, for the LDA volumes correspond to full structural optimization, whereas those reported here are obtained from isotropic volume optimization, which is necessarily more restricted and, hence, less exact. It is equally satisfying that the relative stabilities of these four phases are also very close, with the exception that the order of the fully optimized LDA brookite and colombite phases is correct. Here the difference in energy between the rutile and anatase phases is 0.02–0.06 eV compared with the LDA value of 0.033 eV: both agree well with the experimental enthalpy difference of 0.05 eV reported by Navrotsky and Kleppa (38). For the

TABLE 10
The Calculated Total Energies (Ha) of the FM *Imma* Structure (31) of $LiTiO_2$

Approximation	Energy
UHF	−1005.949841
UHF/PBE	−1007.545192
UHF/PW	−1009.073213
UHF/P	−1007.670266

TABLE 11
Comparison of the Relative Energies (eV) of the Polymorphs of $LiTiO_2$ Based on the Experimental Structures of *Imma* $Li_{0.5}TiO_2$ (31), *Fm*$\bar{3}$*m* $LiTiO_2$ (35), *Pnma* $Li_{0.14}TiO_2$ (15) and *P*4_2/*mnm* TiO_2 (28)

Space group	Volume (Å^3)	UHF	PBE	PW	P
Imma (FM)	35.1360	0.0	0.0	0.0	0.0
Imma (AF)	35.1360	−0.04	−0.04	−0.03	−0.04
Fm$\bar{3}$*m*	35.4790	+0.10	+0.30	+0.24	+0.29
Pnma	35.1014	+1.16	+1.09	+1.11	+1.08
$P4_2/mnm$	31.2175	+3.92[a]	—	—	—

[a]Conducting state.

brookite phase the corresponding RHF and LDA differences are 0.06 and 0.058 eV, respectively.

Mulliken population analyses, which are identical for the experimental and Hartree–Fock structures, show that, despite their differences in volume and local coordination, the six polmorphs have similar electron distributions with effective cation charges of ~2.5 *e* and 3*d* populations of ~1.3 electrons. This suggests a substantial degree of covalency with a significant weight of oxygen states at the lower edge of the conduction band. Figure 9 shows that the upper valence bands are all predominantly O(2*p*) with a small contribution of Ti(3*d*) states across the entire widths which range from ~7.7 eV for the rutile phase to ~6.3 eV for anatase: these compare with superior LDA values of 5.52 and 5.12 eV (37) and experimental widths of 5.4 and 4.75 eV reported by Mo and Ching (36). Lower valence bands of largely O(2*s*) character lie ~14–15 eV below the upper bands, which is in qualitative agreement with experiment (39). The present results are consistent with many other calculations which find Hartee–Fock band widths to be uniformaly greater than experiment (25).

For $LiTiO_2$ there is less scope for detailed comparison with experiment, however, as shown in Table 11, the volumes of the *Imma* and *Pnma* phases based on $Li_{0.5}TiO_2$ are within 1.1% of the volume reported for *Fm*$\bar{3}$*m* $LiTiO_2$ (35), so that in this respect the *Imma* and *Pnma* structures are not unrealistic. For these "experimental" structures the *Imma* phase is predicted to be 0.1 eV lower in energy than *Fm*$\bar{3}$*m* at the UHF level and ~0.3 eV lower including correlation, with a further stabilization of the antiferromagnetic spin arrangement by 0.04 eV per formula unit. The latter compares with previous Hartree–Fock values of 0.06, 0.02, and 0.006 eV for the stabilization of the antiferromagnetic phases in MnO_2 (14), *C*2/*m* $LiMnO_2$ (5), and MnO (11), respectively. The *Pnma* structure is found to be less stable than *Imma* by ~1.1 eV at all levels of approximation and the ground state of $LiTiO_2$ in the unreconstructed rutile structure to be conducting and, as a result, much higher in energy.

TABLE 13
Comparison of the Relative Energies (eV) of the Polymorphs of $LiTiO_2$ for the Hartree–Fock Structures

Space group	UHF	PBE	PW	P
Imma (FM)	0.0	0.0	0.0	0.0
Imma (AF)	−0.02	−0.02	−0.02	−0.02
Fm$\bar{3}$*m*	+0.44	+0.31	+0.41	+0.31
Pnma	$+0.92_5$	+0.96	+0.94	+0.96
$P4_2/mnm$	+0.84	+0.84	+0.84	+0.84

The Hartree–Fock volume of the (known) *Fm*$\bar{3}$*m* phase is ~3.9% greater than that reported (35). This discrepancy is larger than those of the five known polymorphs of TiO_2, which are all close to 1%, but within the errors of Hartree–Fock calculations more generally (38), so that it is unlikey that the neglect of disorder is reponsible for the discrepancy. In the case of *C*2/*m* $LiMnO_2$, with a cation (antisite) disorder of ~10% (6), the Hartree–Fock volume is ~2% greater than experiment. As expected, the Hartree–Fock volumes of the *Imma*, *Pnma*, and $P4_2/mnm$ phases are appreciably greater than those based on $Li_{0.5}TiO_2$ and TiO_2, with increases of 12.8, 15.9, and 24.5%, respectively. Table 13 shows that volume optimization of the *Imma* phase

TABLE 12
Comparison of the Hartree–Fock Volumes (Å^3) of the Polymorphs of $LiTiO_2$ and with Experimental Volumes of Table 11, δv(%)

Space group	Volume	Δv (%)	δv (%)
Imma	39.6374	0.0	+12.81
Fm$\bar{3}$*m*	36.8589	−7.01	+3.89
Pnma	40.6807	+2.63	+15.89
$P4_2/mnm$	38.8679	−1.94	+24.51
$LiMnO_2$	37.7061	—	+1.95

Note. Also given are the volumes and δv for *C*2/*m* $LiMnO_2$ (6).

TABLE 14
Differences in Energy (eV) between the Experimental and Hartree–Fock Structures of the Polymorphs of $LiTiO_2$

Space group	UHF	PBE	PW	P
Imma (FM)	−0.37	+0.10	−0.13	+0.09
Fm$\bar{3}$*m*	−0.04	$+0.11_5$	+0.04	+0.11
Pnma	−0.61	-0.02_5	−0.30	−0.03
$LiMnO_2$	−0.01	+0.06	+0.03	+0.06

Note. Also given are the differences for *C*2/*m* $LiMnO_2$ (6).

TABLE 15

Comparison of the Mulliken Charges, $q_M(x)$ (e), 3d Populations, n_d, and Local Spin Moments, n_s (μ_B), of the Polymorphs of $LiTiO_2$ for the Volume-Optimized Hartree–Fock Structures of Each

Space group	q_M(Li)	q_M(Ti)	$q_M(O_1)$	$q_M(O_2)$	n_d	n_s(Ti)	n_s(O)
Imma (FM)	0.97	2.25	1.64	1.58	1.63	1.01	−0.01
$Fm\bar{3}m$	0.97	2.23	1.59	1.60	1.64	1.01	± 0.02
Pnma	0.95	2.30	1.55	1.70	1.59	1.01	−0.01
$P4_2/mnm$	0.95	2.27	1.60	1.62	1.60	1.01	−0.01

stabilizes it further with respect to $Fm\bar{3}m$ with a difference in UHF energy of 0.44 eV. The *a posteriori* inclusion of correlation is somewhat inconclusive but does not significantly reduce the stability of the *Imma* structure. Volume optimization of the *Pnma* phase leads to a slight increase in stability relative to *Imma*, but is still ~0.9 eV higher in energy, while the Hartree–Fock $P4_2/mnm$ structure, whose volume is ~25% greater than that of TiO_2, is found to be insulating and ~0.1 eV more stable than Pnma. Overall, then, UHF calculations predict the *Imma* phase of $LiTiO_2$ to be the most stable of the four considered here with

$$Imma > Fd\bar{3}m > P4_2/mnm > Pnma.$$

In view of the large differences in volume between the Hartree–Fock and "experimental" structures of the *Imma*, *Pnma*, and $P4_2/mnm$ structures, and complete change of state in the case of the latter, the differences in energy, shown in Table 14, are of limited value, but are included for completeness. However, it is noteworthy that for the $Fm\bar{3}m$ phase the differences in energy are comparable to those for TiO_2 (Table 8) and also $C2/m$ $LiMnO_2$.

While the relative energies of the various polymorphs of TiO_2 and $LiTiO_2$ are, perhaps, of major interest from the electrochemical point of view, in that that they relate directly to (relative) cathodic voltages, as discussed below, differences in the electronic (and magnetic) structures reveal

TABLE 16

Comparison of the *Changes* in the Mulliken charges, $\delta q_M(x)$ (e), 3d populations, δn_d, and Local Spin Moments, δn_s (μ_B), of the Polymorphs of $LiTiO_2$ Compared with TiO_2 for the Volume-Optimized Hartree–Fock Structures of Each

Space group	δq_M(Ti)	$\delta q_M(O_1)$	$\delta q_M(O_2)$	$\delta q_M(O_{tot})$	δn_d	δn_s(Ti)
Imma (FM)	0.07	+0.54	+0.37	0.91	+0.24	+1.01
Pnma	0.05	+0.30	+0.60	0.90	+0.22	+1.01
$P4_2/mnm$	0.22	+0.36	+0.38	0.74	+0.35	+1.01

TABLE 17

A Comparison of Lithium Insertion Energies (eV) for Various Combinations of Polymorphs of TiO_2 and $LiTiO_2$ Based on Their Hartree–Fock structures

	$\langle TiO_2 \xrightarrow{Li} LiTiO_2 \rangle$			
Route	UHF	PBE	PW	P
$P4_2/mnm \rightarrow Imma$	0.0	0.0	0.0	0.0
$Imma \rightarrow Imma$	−0.66	−0.67	−0.66	−0.67
$Pnma \rightarrow Imma$	−0.58	−0.59	−0.59	−0.60
$Imma \rightarrow Pnma$	+0.27	+0.29	+0.28	+0.29
$Pnma \rightarrow Pnma$	+0.35	+0.37	+0.35	+0.36
$P4_2/mnm \rightarrow P4_2/mnm$	+0.84	+0.84	+0.84	+0.84
$P4_2/mmm \rightarrow Pnma$	+0.93	+0.96	+0.94	+0.96

the nature of the fundamental electronic processes associated with lithium insertion. Table 15 contains details of Mulliken population analyses of $LiTiO_2$, and Table 16 shows the *differences* in the various populations between $LiTiO_2$ and TiO_2. From these it is clear that in $LiTiO_2$ lithium is essentially ionic (Li^+) and that in the *Imma* and *Pnma* polymorphs the electron transfer from the inserted lithium to TiO_2 is confined almost exclusively to the oxygen sublattice with less than 10% to the cation sites. In both structures there is an unequal redistribution of charge with the majority localizing on the oxygen sublattice closest to the lithium. However, perhaps the most interesting feature to emerge from the Mulliken analyses is that lithium insertion in TiO_2 to form $LiTiO_2$ leads to a rehybridization of the titanium orbitals leading to an *increase* in the 3d population by ~0.2 e and formation of a local moment of ~1 μ_B at the titanium sites with negligible dispersion on the oxygen sites in both the *Imma* and *Pnma* structures. In the $P4_2/mnm$ structure there is ~20% charge transfer to the cation sublattice with an increase in the 3d population of 0.35 e and, once again, the formation of a local moment

TABLE 18

Calculated Voltages of $TiO_2 \xrightarrow{Li} LiTiO_2$ *Anodic* to $C2/m$ $Li_{0.5}MnO_2 \xrightarrow{Li} LiMnO_2$ Based on Experimental (expt) and Volume-Optimized Hartree–Fock (UHF) Structures of $LiMnO_2$, $Li_{0.75}MnO_2$, and $Li_{0.5}MnO_2$

	$2(LiMnO_2)_{C2/m} + TiO_2 + 2(Li_{0.5}MnO_2)_{C2/m} + LiTiO_2$
Route	Expt/UHF
$P4_2/mnm \rightarrow Imma$	3.20
$Imma \rightarrow Imma$	2.54
$Pnma \rightarrow Imma$	2.62
$Imma \rightarrow Pnma$	3.47
$Pnma \rightarrow Pnma$	3.55
$P4_2/mnm \rightarrow P4_2/mnm$	4.40
$P4_2/mmm \rightarrow nma$	4.13

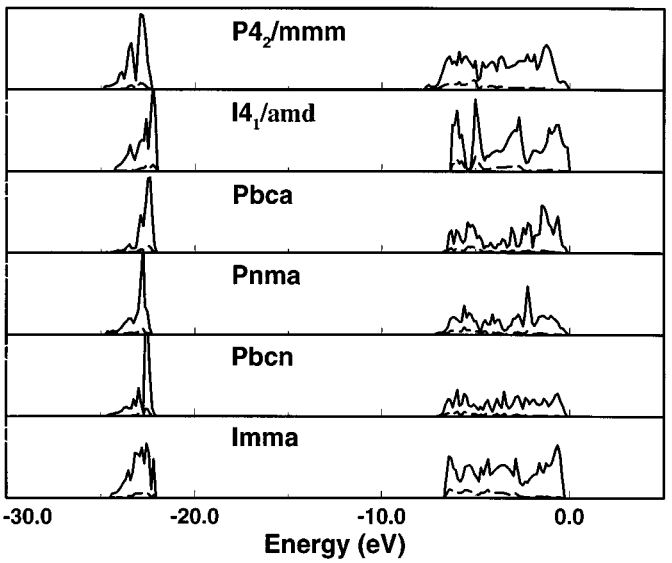

FIG. 9. Valence band densities of states of the polymorphs of TiO_2 (full line, oxygen projections, dashed lines, titanium projections; the zero of energy is placed at the upper edge of the O(2*p*) band).

of $\sim 1\ \mu_B$ at the titanium sites. This bears strong similarities with a previous UHF study of $C2/m$ Li_xMnO_2 (5), in which it was suggested that electron tranfer associated with the *removal* of lithium from $LiMnO_2$ was predominantly from the oxygen sublattice with a reduction of the local moment at the cation sites but strong localization of spin density at the oxygen sites. Thus, UHF calculations predict a change from a nonmagnetic to a magnetic structure on lithium insertion, and while the results reported here apply to $LiTiO_2$, it is speculated that this transition will also take place for much lower levels of lithium insertion. Figure 10 shows that electron transfer leads to the creation of new filled states above the upper valence band edge with weights on both sublattices. These new states are strongly reminiscent of the gap states which have been identified in oxygen-deficient TiO_2 (39) and predicted from UHF calculations (25). Similarly, they should be detectable in Li_xTiO_2. For the *Imma* and *Pnma* structures there are small decreases in the widths of the valence bands which remain predominantly O(2p) in contrast to the $P4_2/mnm$ structure, where a substantial rehybridization of valence orbitals evidently takes place. Equally, electron transfer to oxygen sites leads to a decrease in the empty O(2*p*) states, which, in principle should be detectable by oxygen *k*-edge spectroscopy. However, the broad dispersion of these states might make this difficult.

The differences in stability of the various polymorphs lead to different insertion energies (voltages) depending on the "route" from TiO_2 to $LiTiO_2$. Table 17 lists these energies relative to $P4_2/mnm \xrightarrow{Li}$ Imma, which represents the most stable endpoints. From this three points of interest emerge. The first is that correlation effects, at least at the *a posteriori* level of approximation, are negligible. Second, of the various possibilities, lithiation of the *Imma* phase leads to the largest drop in voltage and via $P4_2/mnm \xrightarrow{Li} Pnma$ the smallest, with a difference of ~ 1.6 eV between them. Third, the $Pnma \xrightarrow{Li} Pnma$ route is predicted to be less facile than $Imma \xrightarrow{Li} Imma$ by ~ 1 eV. It is important to emphasize that the values reported here refer to *complete* lithiation and that

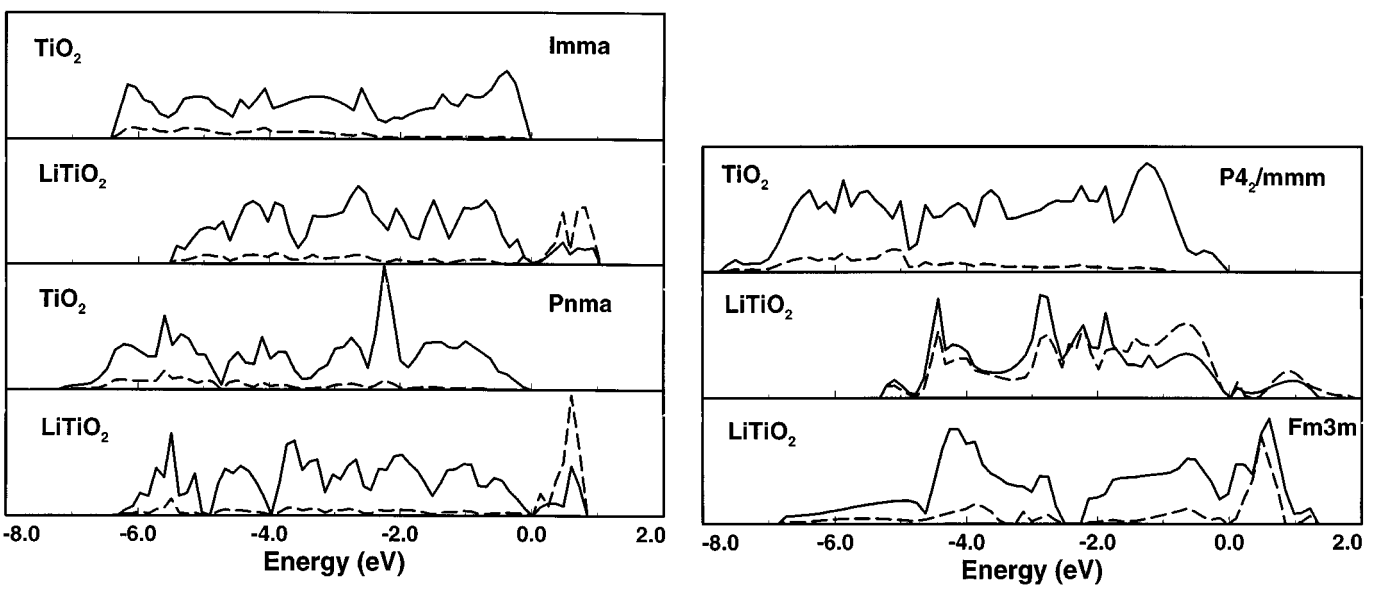

FIG. 10. Comparison of the upper valence band densities of states of the polymorphs of TiO_2 and $LiTiO_2$ (full line, oxygen projections; dashed lines, titanium projections; for both TiO_2 and $LiTiO_2$ the zero of energy is placed, as in Fig. 9, at the upper edge of the O(2*p*) band).

voltages corresponding to more restricted ranges of lithiation might differ from these. However, it seems likely that practical applications of Li_xTiO_2 would utilize as wide a range of lithiation as possible, so that the present estimates might be realistic. Thus, Akimoto *et al.* (15) have demonstrated the *delithiation* of *Pnma* Li_xTiO_2 in the range $0.5 > x \geq 0$, and Gover *et al.* (16), have demonstrated electrochemical cycling over an extended range.

Finally, the calculated stabilities of the polymorphs of TiO_2 and $LiTiO_2$ can be combined with previous UHF results for $C2/m$ Li_xMnO_2 (5) to estimate the *relative* voltage of $TiO_2 \xrightarrow{Li} LiTiO_2$ against $C2/m$ $MnO_2 \xrightarrow{Li} LiMnO_2$. This is a far more consistent procedure, and perhaps more useful, than estimating the voltage against lithium metal since it eliminates the (sizeable) errors of many types that would be involved in combining Hartree–Fock formation energies of $LiTiO_2$ and lithium metal. The $C2/m$ phase is apparently retained down to compositions in the region of $Li_{0.5}MnO_2$, below which there is a structural phase transition to a rhombohedral form (6): accordingly, the relative voltages of $TiO_2 \xrightarrow{Li} LiTiO_2$ against $C2/m$ $Li_{0.5}MnO_2 \xrightarrow{Li} LiMnO_2$ have been estimated based on the experimental structure of $LiMnO_2$ (6) and volume-optimized Hartree–Fock structures of $Li_{0.5}MnO_2$. The calculated voltages agree to less than 0.01 eV for the two structures and are presented in Table 18 as voltages *anodic* to Li_xMnO_2. Armstrong and Bruce (6) have reported an average voltage of $\sim$4 eV cathodic to a carbon-based negative electrode in the upper half of the cycle, from which voltages of $\sim$0.4 and $\sim$1.5 eV cathodic to this same negative electrode can be deduced for the *Pnma* and *Imma* phases of Li_xTiO_2, respectively.

5. CONCLUSIONS

The overall conclusion of this paper is that it confirms the view previously opined in relation to $C2/m$ Li_xMnO_2 (5) that Hartree–Fock methodology can be deployed usefully to investigate the potential electrochemical properties of Li_xTiO_2. This is supported further by the close agreement of the volumes and stabilities of the polymorphs of TiO_2 given here and those reported recently by Milman (37) based on LDA calculations. The specific conclusions are that:

(i) the difference in energy based on experimental and volume-optimized Hartree–Fock structures is less than 0.1 eV for the known polymorphs of TiO_2 and $LiTiO_2$;

(ii) the order of stability of the polymorphs of TiO_2 is

$$P4_2/mnm \text{ (rutile)} > I4_1/amd \text{ (anatase)} > Pbca \text{ (brookite)}$$
$$\approx Pbcn \text{ (high pressure)} > Pnma \text{ (ramsdellite)}$$
$$> Imma > Fd\bar{3}m \text{ (spinel)};$$

(iii) the energy difference between rutile and anatase, 0.02–0.06 eV, is close to that obtained from LDA calculations, 0.033 eV (37), and to the experimental value of 0.05 eV (38)—the corresponding RHF and LDA differences for brookite are 0.06 and 0.058 eV, respectively;

(iv) the *Pnma* (ramsdellite) and *Imma* phases are less stable than $P4_2/mnm$ by $\sim$0.6 eV and the spinel phase by $\sim$1.8 eV;

(v) the order of stability of the polymorphs of $LiTiO_2$ studied here is

$$Imma > Fm\bar{3}m > P4_2/mnm > Pnma;$$

(vi) the (open-circuit) cathodic voltage associated with the complete lithiation of TiO_2 to $LiTiO_2$ via different polymorphic routes might differ by as much as 1.6 eV;

(vii) the largest voltage occurs for the *Imma* route and is $\sim$1 eV greater than that for *Pnma*;

(viii) the voltage for *Imma* Li_xTiO_2 (x: $0 \rightarrow 1$) is *anodic* to $C2/m$ Li_yMnO_2 (y: $0.5 \rightarrow 1.0$) by $\sim$2.5 eV and by $\sim$3.5 eV for the *Pnma* polymorph;

(ix) in $LiTiO_2$ the lithium is essentially ionic (Li^+) and the electron transfer associated with the insertion, $TiO_2 \xrightarrow{Li} LiTiO_2$, is predominantly to the oxygen sublattice(s);

(x) lithium insertion leads to the creation of occupied titanium and oxygen states above the upper valence band edge in a similar fashion to that predicted previously for oxygen loss (25) and should similarly be observable

(xi) the charge transfer to the oxygen sites reduces the density of unoccupied oxygen p states which might be detectable by oxygen k-edge spectroscopy;

(xii) a rehybridization of the titanium (valence) orbitals occurs on lithiation of TiO_2 with an increase in the d-electron population and strong localization of local spin moments of $\sim$1 μB at the titanium sites which should be detectable by polarized neutron diffraction.

ACKNOWLEDGMENT

The author thanks Dr. R.E.Morris for kindly preparing the figures of crystal structures.

REFERENCES

1. G. Pistoia, Ed., "Lithium Batteries. New Materials, Developments and Perspectives." Elsevier, Amsterdam, 1994.
2. P. G. Bruce, *Chem. Commun.*, 1817 (1997).
3. C. R. A. Catlow, Ed., "Computer Modelling in Inorganic Crystallography". Academic Press, San Diego, 1997.
4. G. Ceder, Y. M. Chiang, D. R. Sadoway, M. K. Aydinol, Y. I. Jang, and B. Huang, *Nature* **392,** 694 (1998).
5. W. C. Mackrodt and E.-A. Williamson, *Phil. Mag. B.* **77,** 1077 (1998).
6. A. R. Armstrong and P. G. Bruce, *Nature* **381,** 499 (1996).
7. M. D. Towler, N. L. Allan, N. M. Harrison, V. R. Saunders, W. C. Mackrodt, and E. Aprà, *Phys. Rev. B* **50,** 5041 (1994).

8. M. D. Towler, R. Dovesi, and V. R. Saunders, *Phys. Rev. B* **52,** 10150 (1995).
9. W. C. Mackrodt, N. M. Harrison, V. R. Saunders, N. L. Allan, and M. D. Towler, *Chem. Phys. Lett*. **250,** 66 (1996).
10. W. C. Mackrodt and E.-A. Williamson, *J. Chem. Soc. Faraday Trans.* **92,** 2043 (1996).
11. W. C. Mackrodt and E.-A.Williamson, *J. Phys. Condensed Matter Phys*., **9,** 6951 (1997).
12. W. C. Mackrodt, E.-A. Williamson, D. Williams, and N. L. Allan, *Phil. Mag. B*. **77,** 1063 (1998).
13. P. Kuiper, G. Kruizinga, J. Ghijsen, G. A. Sawatzky, and H. Verweij, *Phys. Rev. Lett*. **62,** 221 (1989).
14. W. C. Mackrodt and E.-A. Williamson, *J. Chem. Soc. Faraday Trans.* **93,** 3295 (1997).
15. J. Akimoto, Y. Gotoh, Y. Oosawa, N. Nonse, T. Kumagni, and K. Aoki, *J. Solid State Chem.* **113,** 27 (1994).
16. R. K. B. Gover, J. R. Tolchard, J. S. T. Irvine, T. Murai, and H. Tukamoto, submitted fo publication.
17. R. Dovesi, V. R. Saunders, C. Roetti, M. Causà, N. M. Harrison, R. Orlando, and E. Aprà, "CRYSTAL 95, User Manual." Università di Torino and CCLRC Daresbury Laboratory, 1995.
18. C. Pisani, R. Dovesi, and C. Roetti, "Hartree-Fock Ab Initio Treatment of Crystalline Systems," Springer-Verlag, Berlin/New York, 1988.
19. J. A. Pople and R. K. Nesbet, *J. Chem. Phys.* **22,** 571 (1954).
20. R. Dovesi, M. Causà, R. Orlando, C. Roetti, and V. R. Saunders, *J. Chem. Phys.* **92,** 7402 (1990).
21. H. J. Monkhorst and J. D. Pack, *Phys. Rev. B* **13,** 5188 (1976).
22. J. P. Perdew, *Phys. Rev. B* **33,** 8822 (1986); **34,** 7406 (1986).
23. J. P. Perdew and Y. Wang, *Phys. Rev*. B **33,** 8800 (1986); **40,** 3399 (1986); **45,** 13244 (1992).
24. J. P. Perdew, K. Burke, and M. Ernzerhof, *Phys. Rev. Lett*. **77,** 3865 (1996); **78,** 1396 (1997); **80,** 891 (1998).
25. W. C. Mackrodt, E.-A. Williamson, and N. M. Harrison, *Surf. Sci*. **384,** 192 (1997).
26. E.-A. Williamson, Ph.D. Thesis, University of St. Andrews (1998).
27. R. S. Mulliken, R. S., *J. Chem. Phys.* **23,** 1833 (1955); **23,** 1841 (1955).
28. C. J. Howard, T. M. Sabine, and F. Dickson, *Acta Crystallogr. B* **47,** 462 (1991).
29. E. P. Meagher and G. A. Lager, *Canad. Mineralogist* **17,** 77 (1979).
30. P. V. Simons and F. Dachille, *Acta Crystallogr.* **23,** 334 (1967).
31. J. R. Cava, D. W. Murphy, and S. Zahurak, *J.Solid State Chem.* **53,** 64 (1984).
32. A. A. Bolzan, C. Fong, B. J. Kennedy, and C.J. Howard, *Austral. J. Chem.* **46,** 939 (1993).
33. C. Fong, B. J. Kennedy, and M. M. Elcombe, *Zeit. Krist*. **209,** 941 (1994).
34. Y. D. Kondrashev and A. I. Zaslavsky, *Izvest. Akad. Nauk SSSR Seriya Fiz*. **15,** 179 (1951).
35. A. Lecerf, *Ann. Chimie* (*Paris*), 513 (1962).
36. S.-D. Mo and W. Y. Ching, *Phys. Rev. B* **51,** 13023 (1995).
37. V. Milman, *in* "Properties of Complex Inorganic Solids" (Proceedings, 1st International Alloy Conference, Athens) (A. Gonis, A. Meike, and P. E. A. Turchi, Eds.), p. 19. Plenum Press, New York, 1997.
38. A. Navrotsky and O. J. Kleppa, *J. Am. Ceram. Soc.* **50,** 526 (1967).
39. K. Prabhakaran, D. Purdie, R. Casanova, C. A. Muryn, and P. J. Hardman, *Phys. Rev. B* **45,** 6969 (1992).
40. R. Dovesi, C. Roetti, C. Freyria-Fava, E. Aprà, V. R. Saunders, and N. M. Harrison, *Phil. Trans. R. Soc. Lond. A* **341,** 203 (1992).
41. R. G. Egdell, S. Eriksen, and W. R. Flavell, *Solid State Commun.* **60,** 835 (1986).